Rapid identification of false peaks in the spectrum of Hadamard transform ion mobility spectrometry with inverse gating technique

Yan Hong,[abd] Wenqi Niu,[c] Hui Gao,[ab] Lei Xia,[a] Chaoqun Huang,[a] Chengyin Shen,[*a] Haihe Jiang[a] and Yannan Chu[*a]

[a] *Laboratory of Medical Optical and Mass Spectrometry, Center of Medical Physics and Technology, Hefei Institutes of Physical Science, Chinese Academy of Sciences, No. 350 Scientific Road, Hefei 230031, China*

[b] *Laboratory of Environmental Spectroscopy, Anhui Institute of Optics and Fine Mechanics, Chinese Academy of Sciences, No. 350 Scientific Road, Hefei 230031, China*

[c] *School of Science, Anhui Agricultural University, Hefei 230036, China*

[d] *School of Electrical and information engineering, Anhui University of Science and Technology, Huainan 232001, China*

Abstract

With the application of Hadamard transform (HT) technique, the signal to noise ratio of ion mobility spectrometry (IMS) has been improved significantly. Nevertheless, possibly due to the modulation defects, the false peaks appear in the demultiplexed data and demonstrate similar features to those of the real signal peaks, which makes them hard to be discriminated. Facing this challenge, a novel method has been presented in this work and achieved the rapid identification of the false peaks in Hadamard multiplexing IMS. Simply by introducing the inverse gating

[*] Corresponding author. Fax: +86 551 65595179
E-mail address: chyshen@aiofm.ac.cn (C. Shen)
[*] Corresponding author. Fax: +86 551 65595311
E-mail address: ychu@aiofm.ac.cn (Y. Chu)

technique to Hadamard multiplexing, the novel inverse Hadamard transform (IHT) method is developed. With the application of this novel method in IMS, most of the false peaks are changed to opposite to the real signal peaks, which makes them easy to be classified as the false peaks. Furthermore, with the help of the single "code " extended method, the amount of the false peaks in inverse Hadamard transform ion mobility spectrometry (IHT-IMS) decreases dramatically, and this makes the identification more accurate. The sample tests further demonstrate that the inverse Hadamard transform (IHT) method is an effective way to address the problem of rapid identification of the false peaks and upgrade the quality analysis of Hadamard multiplexing ion mobility spectrometry.

1. Introduction

In order to enhance the signal to noise ratio (SNR), the Hadamard multiplexing technique was proposed and achieved the increase of the duty cycle (DC) from nearly 1% to 50%. After the application in spectrometer,[1,2] the Hadamard multiplexing has been adopted in many other fields, such as time-of-flight mass spectrometry,[3-6] fluorescence imaging,[7] nuclear magnetic resonance (NMR),[8,9] capillary electrophoretic separations,[10-17] gas chromatography/mass spectrometry (GC/MS),[18-24.] and ion mobility spectrometry,[25-29] etc.

Actually, with the introduction of Hadamard multiplexing technique, the significant enhancement of SNR has been achieved. However, the false peaks appeared in the decoded data of HT technique. Gao et al.[30] found negative peaks in the deconvolution spectrum of Hadamard transform and Fourier transform of mass spectrometry/mass spectrometry and described them as the product of variations of amplitude and frequency of two magnitude modes. Zeppenfeld et al.[31] concluded that the negative systematic errors were caused by the instrumentation in time of flight analysis. In terms of other application of Hadamard multiplexing, [15-17,18] the demultiplexed data also contain false peaks and most of them are characterized as negative peaks. Due to their negative features, these kind of false peaks are relatively easy to be identified.

Similarly, the false peaks were also presented in Hadamard transform ion mobility spectrometry (HT-IMS).[25,26,28] Furthermore, most of these false peaks demonstrated similar features to those of the real signal peaks, which made them hard to be discriminated. In addition, different constructions of PRBS would lead to different positions and intensities of the false peaks, which made the identification and reduction of the false peaks more complicated.[32] Clowers et al.[25] presented the "doubling" method, which could partially correct the distortion of the HT-IMS. Kwasnik et al.[28] developed an extended HT technique, which achieved the reduction of the false peaks in the demultiplexed data significantly. Prost et al.[29] proposed an algorithm to identify and remove artifacts in the spectra of Hadamard transform ion mobility mass spectrometry (HT-IM-MS), and this algorithm is working under the platform of IM-MS.

In this research, to realize rapid identification of the false peaks in Hadamard multiplexing IMS, a novel inverse Hadamard transform (IHT) method is proposed and applied to IMS. Through comparison the spectra of IHT-IMS and conventional HT-IMS, the effect of this novel method on the false peaks is evaluated. In addition, in order to further enhance the accuracy of the identification, the combination of extended method and IHT-IMS is developed and investigated.

2. Methodological

2.1 Conventional and inverse IMS

Traditionally, the single injection pattern was adopted in conventional IMS. That is, during the total scan time, the ions are injected only once, and the normal gating pulse is adopted. For instance, if the modulation sequence is "1000000000…", the ion gating pulse sequence will be "1000000000…", each "1" corresponds to opening the ion gate for a short time and each "0" means shuttering the ion gate for a short period. The ion mobility spectrum will be obtained after a single injection, as shown in Fig. 1a.

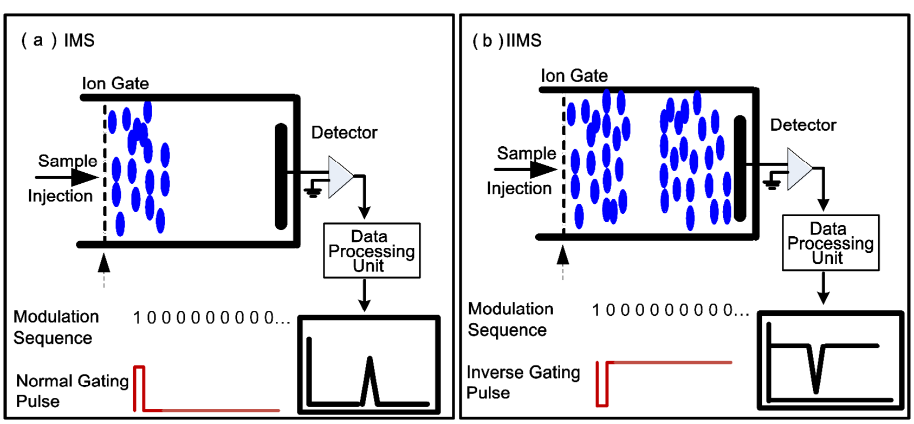

Fig. 1 Schematic diagram of conventional IMS and inverse IMS (IIMS): (a) Working principle for IMS; (b) Working principle for IIMS.

On the contrary, under inverse IMS, first proposed by Tabrizchi,[33] the inverse gating technique is used. Under this mode, the ion gate is always opened except for a short period of gating. Namely, if the modulation sequence is "1000000000…", the ion gating pulse sequence will be "01111111111…". Thus, the inverse ion mobility spectrum will be obtained by a single gating, as shown in Fig. 1b.

2.2 Conventional and Inverse HT-IMS

In order to increase the duty cycle and enhance the SNR of IMS, the Hadamard transform technique was introduced.[25,26,28,29] In conventional Hadamard transform method, the pseudo random binary sequence (PRBS) is used as the modulation sequence, and the normal gating technique is adopted. That is, if a 15-bit PRBS is like "001000111101011", the ion gating pulse sequence will be "001000111101011". Each "0" corresponds to shuttering the injection of the ions for a short period, and each "1" represents activating one injection. Thus the convolution of the conventional Hadamard multiplexing is shown in Eq. 1.

$$[\boldsymbol{Y}] = [\boldsymbol{S}] \times [\boldsymbol{X}] \quad (1)$$

Where S is the $n \times n$ (n is the length of PRBS) matrix, generated by PRBS, and X is a series of data representing a single spectrum derived from a single injection, matrix Y is the convolution spectrum, encoded by multiple normal spectra. To reconstruct the original signal X, the superimposed signal is decoded by multiplication of the inverse S-matrix, S^{-1}, which is shown in Eq. 2. The working principle for HT-IMS is shown in Fig. 2a.

$$[\boldsymbol{X}]^{*} = [\boldsymbol{S}]^{-1} \times [\boldsymbol{Y}] = [\boldsymbol{S}]^{-1} \times [\boldsymbol{S}] \times [\boldsymbol{X}] \quad (2)$$

In this research, through inversing the gating pulse of conventional Hadamard multiplexing, the inverse Hadamard transform (IHT) method is designed and applied to ion mobility spectrometry. Under IHT mode, the PRBS is still working as the modulation sequence, but the normal gating pulse used in HT mode is substituted by the inverse gating technique. That is, if the modulation sequence is "001000111101011…", the ion gating pulse sequence will be "110111000010100…". Thus the convolution of inverse mode Hadamard multiplexing could be described as Eq. 3.

$$[\boldsymbol{Y}_1] = [\boldsymbol{S}_1] \times [\boldsymbol{X}_1] \quad (3)$$

Where X_1 represents a series of data corresponding to a single gating, S_1 represents the S-matrix, and Y_1 is the convolution of inverse mode Hadamard multiplexing, which is superimposed by multiple inverse spectra. Despite of different form of gating techniques, the modulation sequence of IHT mode is the same with that of the conventional HT mode. As a result, the encoding S-matrix used in IHT mode will keep the same with that of conventional HT mode. That means S_1 is equal to S, thus the decoded process could be described as Eq. 4.

$$[\boldsymbol{X}_1]^{*} = [\boldsymbol{S}_1]^{-1} \times [\boldsymbol{Y}_1] = [\boldsymbol{S}]^{-1} \times [\boldsymbol{S}] \times [\boldsymbol{X}_1] \quad (4)$$

Where S_1^{-1} represents the inverse matrix of S_1, Y_1 is the convolution of inverse Hadamard transform, X_1^{*} represents the recovered inverse spectrum. The design of IHT-IMS is shown in Fig. 2b.

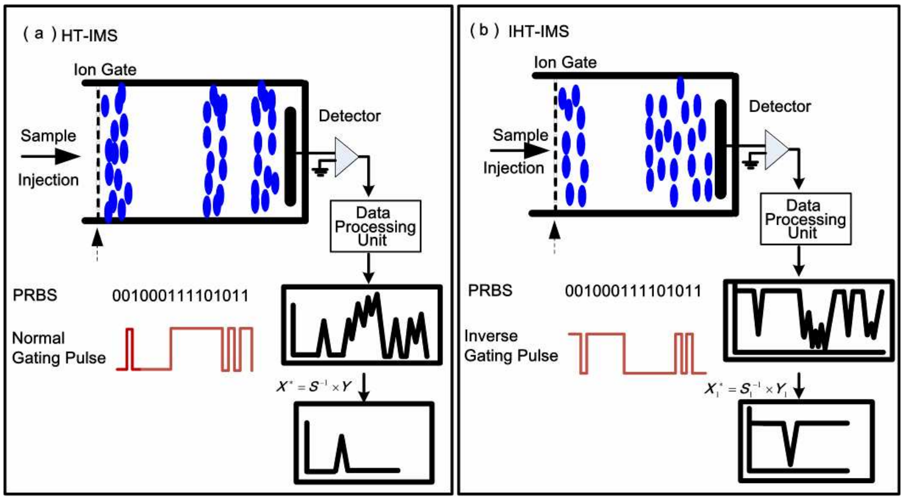

Fig. 2 Schematic diagram of conventional HT-IMS and IHT-IMS: (a) Working principle for HT-IMS; (b) Design of IHT-IMS.

3. Experimental

The schematic diagram of our home-built atmospheric pressure corona discharge ion mobility spectrometry (APCD-IMS) is shown in Fig. 3. It consists of ion drift tube (including ionization region, reaction region, ion gate, drift region and Faraday plate), ion gate controller, data processing unit and high-voltage power supply module (HV). The reaction region and drift region are insulated by a B-N ion gate, which is coupled with ion gate controller. Under the control of the ion gate controller, the ion gate is opened or shuttered, which releases or prevents the ion packets into the drift region. With the output of the ion gate control sequence, the synchronous signal (SYN, shown in Fig. 3) will be generated and reach the data processing unit to trigger the data acquisition periodically.

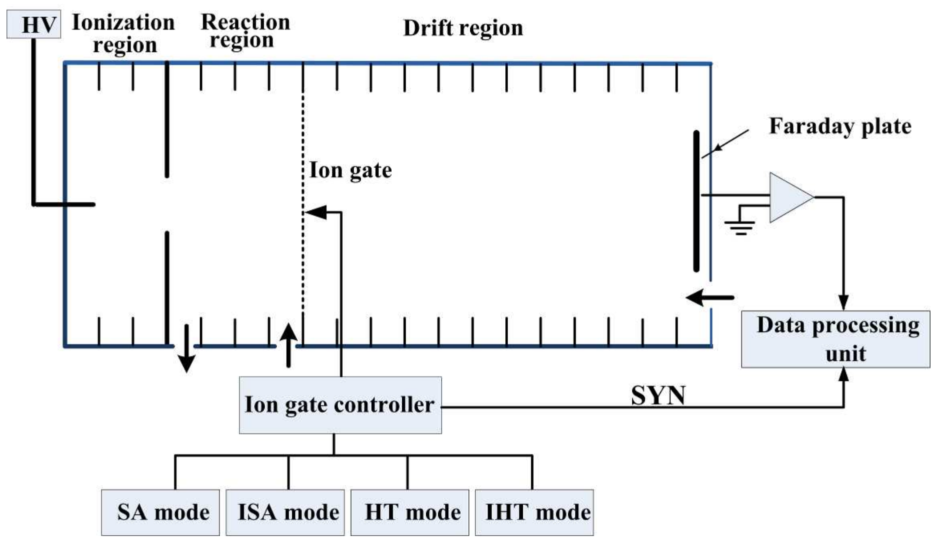

Fig. 3 Schematic diagram of atmospheric pressure corona discharge ion mobility spectrometer (APCD-IMS)

The ion gate controller can work under four modes, they are conventional signal averaging mode (SA mode), conventional Hadamard transform mode (HT mode), inverse signal averaging mode (ISA mode) and inverse Hadamard transform (IHT mode), respectively. In this work, the IMS works under negative detection mode.

4. Results and discussion

4.1 Discriminating the false peaks

To simplify the analysis, no sample gases are injected into APCD-IMS except for the ambient air. The reactant ions ($O_2^-(H_2O)_n$) are generated in the ionization region through negative corona discharge in air. Because no sample molecules are injected into the APCD-IMS, the measurement is mainly about the reactant ions ($O_2^-(H_2O)_n$). The homogeneous electric field in the drift region is 300 Vcm^{-1}, the ion gate pulse width for all the experiments is 200 μs.

Fig. 4a demonstrates the spectra of SA-IMS and ISA-IMS. Under SA mode shown in the top of Fig. 4a, the normal reactant ion peak (RIP) is illustrated. Under ISA mode shown in the bottom of Fig. 4a, the inverse reactant ion peak is presented. In terms of the normal and inverse RIPs, although their orientations are opposite, their drift time is the same, which means they symbolize the same kind of ion. However, the intensity of the inverse RIP is lower than that of the normal one. This phenomenon is consistent with the report of Tabrizchi.[33] Through broadening the pulse width, the lower intensity of inverse dip could be compensated,[33] but it would lead to the reduction of the resolution and increase of the time cost. As a result, in this work, we never adjust the gating pulse width for inverse mode.

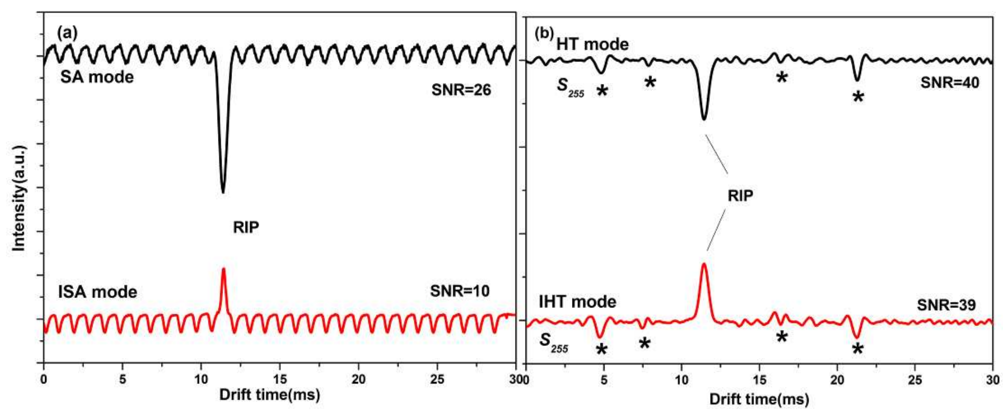

Fig. 4. The spectra obtained by SA mode and HT mode in our home-built APCD-IMS: (a) SA mode and ISA mode, (b) HT mode and IHT mode (the order of S-matrix is 255)

Fig. 4b shows the spectra of HT-IMS and IHT-IMS, the order of S-matrix is 255. Apparently, compared with the SA-IMS, the signal to noise ratio of HT-IMS has been improved significantly. However, in the spectrum of conventional HT-IMS as shown in the top of Fig. 4b, the suspicious false peaks (labeled with asterisk) appear in the demultiplexed data. As discussed previously, the false peaks in HT-IMS were also demonstrated in other reports,[25,26,28] the authors speculated that the imperfect ion gate response, [25] the depletion between adjacent spaced gating events and the thermal or space charge induced diffusion[28] may all contribute to the generation of the false peaks in HT-IMS. However, until now, the specific reasons for the false peaks of HT-IMS have not been given. Additionally, as shown in the spectrum of HT-IMS, most of the false peaks head in the same direction with that of the RIP, which makes them hard to be discriminated from the real signal peaks. As a result, the quality analysis of HT-IMS will be degraded.

On the other hand, the spectrum of IHT-IMS is presented in the bottom of Fig. 4b, the order of the S-matrix is 255, and the gating pulse width is the same with that of the conventional HT method. Different from the result of HT-IMS, the RIP is symbolized by the inverse peak in IHT-IMS, while the suspicious false peaks (labeled with asterisk) in the spectrum of IHT-IMS are kept unchanged. As a result, the suspicious false peaks in IHT-IMS demonstrated different features from the RIPs, which makes them easy to be determined as the false peaks.

Through comparison the spectra of HT and IHT modes as shown in Fig. 4b, it is obvious that the RIPs under two modes are opposite, while the phases of the false peaks under two modes are kept unchanged. As discussed previously, the false peaks in HT-IMS possibly result from the modulation defects.[25,28] As we discussed in the methodology, the modulation sequences for HT and IHT methods are the same, which may lead to similar modulation defects and thus the similar false peaks. Actually, the false peaks in IHT mode are much similar to those of the HT mode, and they are oriented to the same direction with that of the real ion peaks. However, due to opposite ion gating method, the orientation of the signal peaks of IHT mode are opposite to that of the HT mode. All of the above reason might account for the different relationships between false peaks and real signal peaks under HT and IHT modes. Due to different phases of the false peaks and the signal peaks, the rapid identification of the false peaks becomes easy to be accomplished with IHT mode rather than HT mode. Furthermore, this achievement does not need any modification of the instrument and additional computational costs.

4.2 Reducing the false peaks

As demonstrated in Fig. 4b, the problem of identification of the false peaks in Hadamard multiplexing could be addressed by IHT method. However, too many false peaks are located in the demultiplexed data, which would increase the complexity of the determination, especially when multiple components were measured. In order to reduce the false peaks and make the identification more accurate, the combination of the IHT technique and extended method is proposed in this work.

As shown in Fig. 5, the spectra are obtained by extended HT and IHT methods, the order of S-matrix is 255, and single “zero” is appended to each element of the PRBS. Apparently, compared with HT method, the total amount of false peaks declines significantly and only one false peak appears at 21.25 ms under extended HT or IHT modes. As shown in the top of Fig. 5, the suspicious peak (labeled with asterisk) under extended HT mode is still heading the same phase with that of the RIP and hard to be determinated as the false peak. However, under extended IHT mode shown in the bottom of Fig. 5, the suspicious peak (labeled with asterisk) is changed to opposite to that of the RIP (inverse dip). So, under the help of the extended method, the identification of the false peaks in IHT-IMS becomes more accurate.

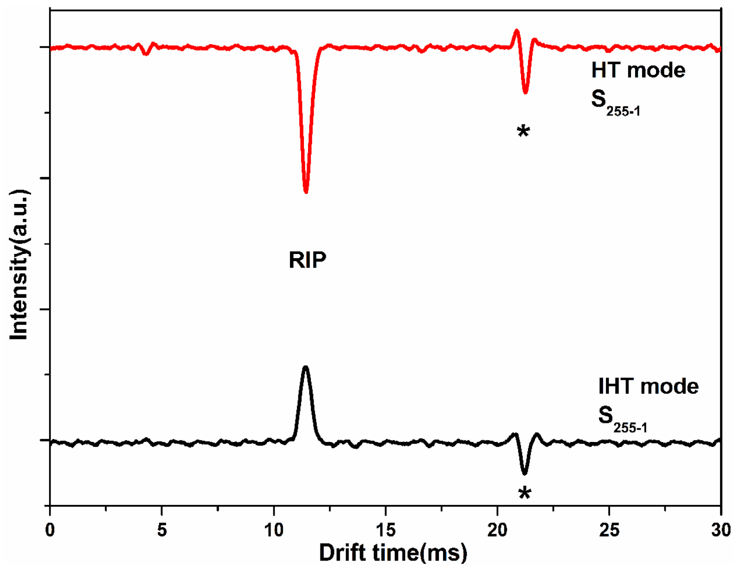

Fig. 5. The spectra are obtained under HT and RHT modes with extended method (the order of S-matrix is 255, single “zero” is appended to each element of the PRBS, denoted as S_{255-1})

On the other hand, it is worth mentioning that when single “code” is adopted in extended IHT method, the total scan time will be doubled. Namely, if the order of the S-matrix is 255, the gating pulse width is 200 μs, the total encoding time of HT-IMS will be about 51 ms, and the time consumption for the data processing (sampling, A/D conversion, decoding, data presentation) will be about 1.5 s, while under single code extended HT method, the order of the modulation matrix will be doubled (from original 255 to current 510), the total encoding time will be doubled (102 ms), thus the time cost for data processing will be about 3 s. As a result, if more extended codes were appended, the time cost for extended HT method would be multiplied, and thus the fast detection speed of the IMS will be affected seriously. Taking these into consider, the single code extended method was selected in our extended inverse Hadamard transform method, which could achieve accurate identification of the false peaks without largely increasing the time cost.

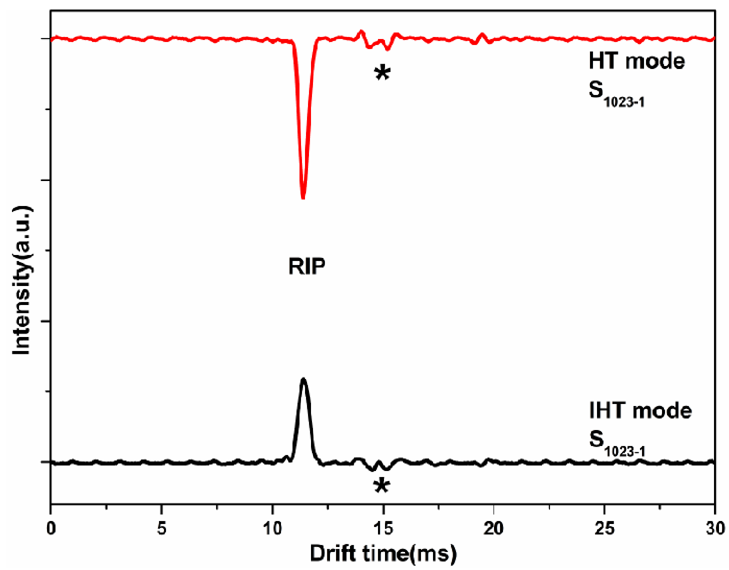

Fig. 6. The spectra are obtained under HT and IHT modes with extended HT method (the order of S-matrix is 1023, and single "zero" is appended to each element of the PRBS, denoted as $S_{1023\text{-}1}$)

To reduce the false peaks further, we try to prolong the order of S-matrix. The spectra in Fig. 6 are obtained under HT and IHT modes with extended method, and the order of S-matrix is 1023 and single "code" is inserted after each element of the PRBS. The results show that the obvious false peak (labeled with asterisk) in Fig. 5 disappears here. Only a minor false peak appears at 15 ms under HT or IHT modes. Furthermore, this false peak is opposite to that of the inverse RIP and easy to be discriminated. The experimental results demonstrate that different modulation sequence may lead to different location of the false peaks, which would increase the complexity of the identification of the false peaks in HT-IMS. Besides, with the single "code" extended IHT method, we could achieve effective reduction and accurate identification of the false peaks in Hadamard multiplexing IMS.

4.3 Sample detection

Measurement of CCl_4

In this section, to evaluate the effect of this novel IHT method, the home-built atmospheric pressure nitrogen corona discharge electron attachment ion mobility spectrometry (APNCD-EA-IMS), described previously by Feng,[34] is adopted. At the same time, the carbon tetrachloride CCl_4 sample is introduced into the reaction region. In the ionization region, the electrons are generated via negative corona discharge in pure nitrogen. In the reaction region, under the function of electron attachment reactions, the negative Cl^- ions are produced during the introduction of CCl_4 (1.15ppm) molecules. Under the control of ion shutter, the ions are released into the drift region accordingly. Under the function of the uniform electric field of 490 Vcm^{-1} in the drift region, the ion mobility spectrum, which contains the electron peak (near zero drift time) and Cl^- peak, will be obtained.

The spectra of HT and IHT mode are demonstrated in Fig. 7, the order of S-matrix is 255, and the gating pulse widths for two modes are still set as 200 μs. Under HT mode as shown in the top of Fig. 7, most of the false peaks (labeled with asterisk) head in the same direction with that of the product ion peak (Cl^-) and the electron peak (*e*), while under IHT mode shown in the bottom of Fig. 7, the false peaks head in the opposite phase with that of Cl^- peak and the electron peak (*e*). Furthermore, the amount of the false peaks (labeled with asterisk) under HT method is slightly more, thus the extended method is associated.

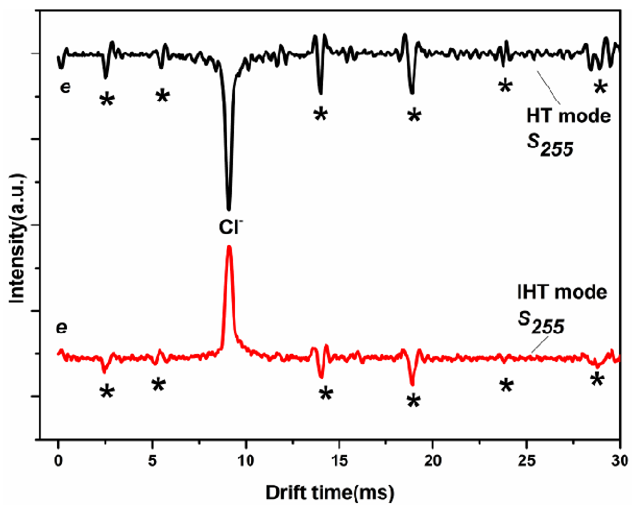

Fig. 7 Measurement of Cl^- with HT and IHT modes (the order of S-matrix is 255)

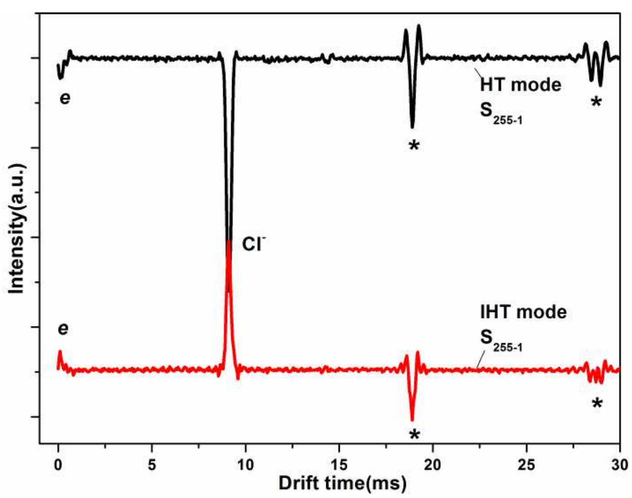

Fig. 8 Measurement of Cl^- under extended HT and IHT modes. The order of S-matrix is 255, the single code extended HT mode is tested and denoted as S_{255-1}.

As shown in Fig. 8, compared with HT mode, the false peaks in extended HT mode (appending one “zero” to each element of PRBS) reduces significantly. Under extended HT mode shown in the top of Fig. 8, the false peak (labeled with asterisk) heads in the same direction with that of the product ion peak (Cl^-) and electron peak (*e*). However, under extended IHT method shown in the bottom of Fig. 8, the false peak has been changed to opposite to the inverse Cl^- peak and electron peak. As a result, with the extended IHT-IMS, the false peaks could be significantly decreased and thus makes the discrimination of the false peaks more accurate.

Measurement of CH_2Br_2

To further verify the effect of this method, the measurement of CH_2Br_2 has been investigated. Similar to the measurement of CCl_4, the high pure nitrigion (99.99%) was injected into the ionization region of APNCD-EA-IMS to produce electrons. The sample dibromomethane CH_2Br_2 (7.6ppm) is introduced into the reaction region and the product ions $Br^-(H_2O)_n$ and $Br_2^-(H_2O)_n$ are generated under the function of electron attachment reactions. The experimental results of conventional IMS, HT-IMS and IHT-IMS are demonstrated in Fig. 9.

Fig. 9a is the spectrum of conventional IMS. “1” and “2” represents the $Br^-(H_2O)_n$ and $Br_2^-(H2O)_n$, respectively. In addition, the electron peak is located near at 0 ms. Fig. 9b is the spectrum of HT-IMS, the order of S-matrix is 255, the product ions (labeled with “1” and “2”) are still located in the spectrum, however, many false peaks (marked with asterisk) appeared. Furthermore, these false peaks own the same phase with that of the product ion peaks ($Br^-(H_2O)_n$ and $Br_2^-(H_2O)_n$), which makes them hard to be distinguished from the real signal peaks. Fig. 9c illustrates the spectrum of

IHT-IMS. The inverse peaks (labeled with “1” and “2”) also symbolize the product ions $Br^{-}(H_2O)_n$ and $Br_2^{-}(H_2O)_n$, respectively. Apparently, under IHT mode, most of the false peaks (labeled with asterisk) are heading the opposite direction to the real signal peaks, which makes them relatively easy to be identified and discriminated.

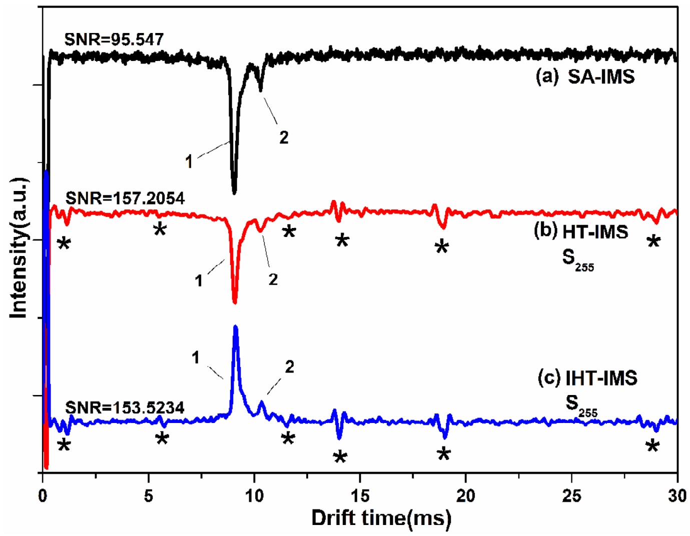

Fig. 9 Measurement of CH_2Br_2 with SA, HT and IHT modes (the order of S-matrix is 255)

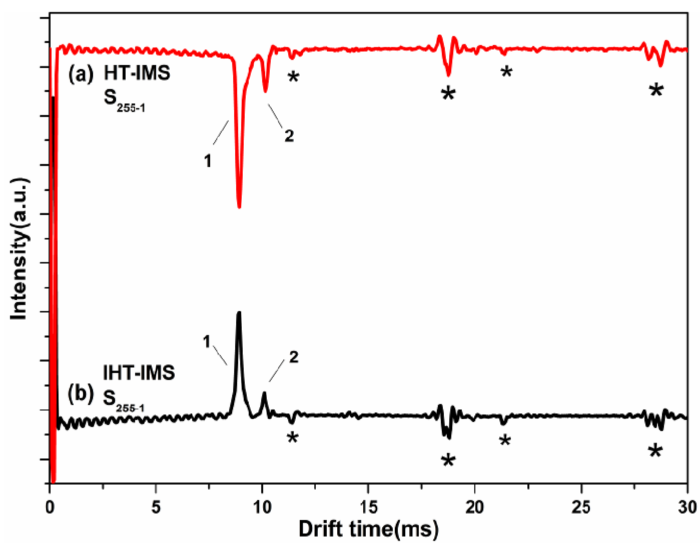

Fig. 10 Measurement of CH_2Br_2 under extended HT and IHT modes. The order of S-matrix is 255, the single code extended HT method is denoted as $S_{255\text{-}1}$.

As shown in Fig. 10, the experimental results of extended HT-IMS and IHT-IMS are given. Under the aid of single code extended method, the amount of false peaks (labeled with asterisk) in the spectra of HT-IMS and IHT-IMS reduces substantially. On the other hand, under extended HT mode shown in Fig. 10a, most of the false peaks are still heading the same direction with that of the signal peaks, however, under extend IHT mode shown in Fig. 10b, the false peaks are opposite to the reverse product ion peaks (labeled with “1” and “2”) and easy to be identified as the spurious peaks.

5. Conclusion

In this work, to achieve rapid identification of the false peaks and enhance the quality analysis of HT-IMS, the novel inverse Hadamard transform (IHT) method is developed by inversing the gating pulse of Hadamard multiplexing. With the application of IHT method in IMS, the different phases are demonstrated between the false peaks and the real signal peaks, and thus make it easy to identify the false peaks from the demultiplexed data. Additionally, with the combination of single code extended technique, the amount of false peaks in IHT-IMS decreases significantly, and this makes the identification more accurate. In summary, this work gives an alternative way to identify the false peaks in Hadamard multiplexing IMS. Furthermore, this method doesn’t need any modification of the hardware structure and the help of additional complicated algorithms, which makes it potentially useful for other similar techniques.

Acknowledgements

This work is supported by the National Natural Science Foundation of China (21403245, 21477132), the Anhui Provincial Program for Science and Technology Development, China (1301042095) and the Innovative Program of Development Foundation of Hefei Center for Physical Science and Technology, China (2014FXCX007).

References

[1] N.M. Larson, R. Crosmun and Y. Talmi, Appl. Optics , 1974, 13, 2662.

[2] N.J.A. Sloane and M. Harwit, Appl. Optics, 1976, 15, 107.

[3] A. Brock, N. Rodriguez and R.N. Zare, Anal. Chem., 1998, 70, 3735.

[4] J.R. Kimmel*, F.M. Fernandez and R.N. Zare, J. Am. Soc. Mass Spectrom., 2003, 14, 278.

[5] F.M. Fernandez, J.M. Vadillo, F. Engelke, J.R. Kimmel, R.N. Zare, N. Rodriguez, M. Wetterhall and K. Markides, J. Am. Soc. Mass Spectrom., 2001, 12, 1302.

[6] R.N. Zare, F.M. Fernandez and J.R. Kimmel, Angew. Chem.-Int. Edit., 2003, 42, 30.

[7] K. Hassler, T. Anhut and T. Lasser, Appl. Optics, 2005, 44, 7564.

[8] J. Ashida, E. Kupce and J.P. Amoureux, J. Magn. Reson., 2006, 178, 129.

[9] H.P. Ke, H.H. Cai, S.H. Cai, H. Chen, Y.Q. Lin and Z. Chen, Chem. Phys., 2014, 444, 61.

[10] J.N. Vandermoolen, D.J. Louwerse, H. Poppe and H.C. Smit, Chromatographia, 1995, 40 368.

[11] T. Kaneta, Y. Yamaguchi and T. Imasaka, Anal. Chem., 1999, 71, 5444.

[12] T. Kaneta, Anal. Chem., 2001, 73, 540A.

[13] T. Kaneta, K. Kosai and T. Imasaka,Anal. Chem., 2002, 74, 2257.

[14] T. Kaneta, K. Kosai and T. Imasaka, Anal. Sci., 2003, 19, 1659.

[15] K. Hata, T. Kaneta and T. Imasaka, Anal. Chem., 2004, 76, 4421.

[16] K.L. Braun, S. Hapuarachchi, F.M. Fernandez and C.A. Aspinwall, Anal. Chem., 2006, 78, 1628.

[17] K. Hata, T. Kaneta and T. Imasaka, Anal. Chim. Acta, 2006, 556, 178.

[18] C.H. Lin, T. Kaneta, H.M. Chen, W.X. Chen, H.W. Chang and J.T. Liu, Anal. Chem., 2008, 80, 5755.

[19] C.C. Cheng, H.W. Chang, T. Uchimura, T. Imasaka, T. Kaneta and C.H. Lin, J. Sep. Sci., 2010, 33, 626.

[20] Y.K. Cheng, C.H. Lin, T. Kaneta and T. Imasaka, J. Chromatogr. A, 2010, 1217, 5274.

[21] Z.Z. Fan, C.H. Lin, H.W. Chang, T. Kaneta and C.H. Lin, J. Chromatogr. A, 2010, 1217, 755.

[22] Y.K. Cheng, C.H. Lin, S. Kuo, J.T. Yang, S.Y. Hsiung and J.L. Wang, J. Chromatogr. A, 2012, 1220, 143.

[23] G.T. Fan, C.L. Yang, C.H. Lin, C.C. Chen and C.H. Shih, Talanta, 2014, 120,

386.

[24] O. Trapp, LC GC Eur., 2011, 24, 172.

[25] B.H. Clowers, W.F. Siems, H.H. Hill and S.M. Massick, Anal. Chem., 2006, 78, 44.

[26] A.W. Szumlas, S.J. Ray and G.M. Hieftje, Anal. Chem., 2006, 78, 4474.

[27] Y.I. Fang, W.Q. Niu, C.Y. Shen, S. Liu, C.Q. Huang, H.M. Wang, H.H. Jiang and Y.N. Chu, Chinese Journal of Quantum Electronics, 2013, 30, 524.

[28] M. Kwasnik, J. Caramore and F.M. Fernandez, Anal. Chem., 2009, 81, 1587.

[29] S.A. Prost, K.L. Crowell, E.S. Baker, Y.M. Ibrahim, B.H. Clowers, M.E. Monroe, G.A. Anderson, R.D. Smith and S.H. Payne, J. Am. Soc. Mass Spectrom., 2014, 25, 2020.

[30] X.L. Gao and T.D. Wood, Rapid Commun. Mass Spectrom., 1996, 10, 1997.

[31] P. Zeppenfeld, M. Krzyzowski, C. Romainczyk and R. David, Rev. Sci. Instrum., 1993, 64, 1520.

[32] J.W. Hudgens and D.E. Bergeron, Rev. Sci. Instrum., 2008,79, 014102.

[33] M. Tabrizchi and E. Jazan, Anal. Chem., 2010, 82, 746.

[34] H.T. Feng, W.Q. Niu, H.Y. Han, C.Q. Huang, H.M. Wang, J. Matuska, M. Sabo, S. Matejcik, H.H. Jiang and Y.N. Chu, INT J MASS SPECTROM, 2011, 305, 30.